A Hybrid Compensator Configuration for VAR Control and Harmonic Suppression in All-Electric Shipboard Power Systems

Terriche, Yacine; Mutarraf, Muhammad Umair; Golestan, Saeed; Su, Chun-Lien; Guerrero, Josep M.; Vasquez, Juan C.

Published in:
I E E E Transactions on Power Delivery

DOI (link to publication from Publisher):
10.1109/TPWRD.2019.2943523

Publication date:
2020

Document Version
Accepted author manuscript, peer reviewed version

This article has been accepted for publication in a future issue of this journal, but has not been fully edited. Content may change prior to final publication. Citation information: DOI 10.1109/TPWRD.2019.2943523, IEEE Transactions on Power Delivery

A Hybrid Compensator Configuration for VAR Control and Harmonic Suppression in All-Electric Shipboard Power Systems

Yacine Terriche, *Student Member, IEEE,* Muhammad Umair Mutarraf, *Student Member, IEEE,* Saeed Golestan, *Senior Member, IEEE*, Chun-Lien Su, *Senior Member*, *IEEE*, Josep M. Guerrero, *Fellow, IEEE*, Juan C. Vasquez, *Senior Member*, *IEEE*, Djallel Kerdoun

***Abstract*—This paper proposes a cost-effective compensator to suppress harmonics and compensate the power factor of all-electric shipboard power systems (SPSs). This compensator, which is based on a fixed capacitor-thyristor controlled reactor (FC-TCR), behaves as a low-pass filter and therefore can reject both low and high-order harmonics. Moreover, the FC-TCR compensator is featured by the low switching losses; hence, it can effectively be implemented for low and medium voltage applications. The design of the filter is detailed via equivalent lossy circuits, which exhibit the mechanism of the harmonic mitigation. Furthermore, theoretical analyses and mathematical developments are suggested to enhance the filtering performance. Besides, details of the Fixed-Point iteration technique which is applied to extract the firing angle of the TCR are conducted. A practical SPS is selected to ensure and demonstrate the performance of proposed methodology via thorough simulations under MATLAB/Simulink environment. The obtained results verify the theoretical analyses and confirm the effectiveness of proposed solution.**

***Index Terms*— Fixed capacitor-thyristor controlled reactor, harmonics, power factor, shipboard power system.**

I. INTRODUCTION

From the early of the last decades, the installation of power electronic converters (PECs) onboard shipboard power systems (SPSs) has been witnessing a substantial evolution [1], [2]. This advance has provided several benefits to all-electric-ship electrical power systems (EPCs), such as easy and fast maneuverability, better efficiency and controllability, faster dynamic response, etc [3]. However, the implementation of PECs, such as variable-voltage-variable-frequency drives, AC-DC converters and other types of non-linear loads, introduces a severe source of harmonics, which affects the EPS operation, and in case of emergency situations threats the lives of the ship crew/passengers, as well as increases the specific emissions [1], [2], [4]. The SPS is arguably a self-sufficient microgrid (MG) which compromises a high resemblance to terrestrial MGs, thus power quality (PQ) solutions that are applied for terrestrial MGs might be effective for SPSs with respect to some SPSs' constraints in terms of physical size, price, and power rating, etc.

The traditional solutions for PQ problems are restricted to some limitations such as the cost, size, power rating, etc. For example, the passive power filters (PPFs) are broadly used to suppress the most dominant harmonics and compensate for some amount of power factor (PF) [5],[6]. They are also characterized by the ease of implementation and maintenance, as well as low-cost. Nonetheless, these filters cannot be a reliable solution for SPSs due to several weaknesses mainly: the size and the weight (bulky), fixed tuning (i.e., they provide a poor performance under frequency variation), fixed reactive power compensation, switching of the stages, etc. The shunt active power filter (SAPF) can overcome the defects of the PPFs [7], [8], [9]. However, for all-electric-ship medium and high power applications, their applications are limited because of their high switching losses and high implementation cost. Furthermore, if the total harmonic distortion (THD) of the voltage exceeds a certain limit ($THD_V > 0.08$-0.1) it can shorten the lifetime of the DC link capacitor [1], [10]. Hybrid APFs (PPFs in series with APFs) can be a good solution to minimize the power rating of the APF [7], [11]. However, since the PPFs are tuned at the most dominant harmonics, it becomes difficult to compensate for high-order harmonics. Furthermore, the parameters of the PPFs change under frequency drifts, which increases the risk of the harmonic resonance and degrades the harmonic compensation. A cost–effective topology is proposed in [10] to overcome some weaknesses of the traditional solutions. This topology, which is based on FC-TCR, can act as a harmonic filter (HF) and at the same time, it can also act as a variable PF compensator. The LC filter, which is installed in series with the main impedance, forces the harmonics to flow through the FC, while the TCR adjusts the PF towards unity. Since the thyristors' valves require only one pulse every half cycle (less switching losses compared to APFs), and the compensator is able to filter low- and high-order harmonics, this solution could be very efficient for ship medium and high power applications. However, the series LC filter might cause a severe drop voltage under frequency drifts and cause a resonance at the terminals of each component. This resonance might not be significant at low power as provided in [10]. However, in medium and high power applications, this resonance increases significantly and leads to hazard coincidences.

In order to maintain the operation security and efficiency of the SPSs, an improved topology of the FC-TCR compensator

Y. Terriche, M. U. Mutarraf, S. Golestan, J. M. Guerrero, and Juan C. Vasquez, are with the Department of Energy Technology, Aalborg University, Aalborg 9220, Denmark. (E-mail: yte@et.aau.dk; mmu@et.aau.dk; sgd@et.aau.dk; joz@et.aau.dk; juq@et.aau.dk)

C. L. Su is with the Department of Marine Engineering, National Kaohsiung University of Science and Technology, Kaohsiung, Taiwan. (E-mail: cls@nkust.edu.tw)

D. Kerdoun is with the Departement of Electrical Engineering, University of Mentouri, 8JRC+84 Constantine, Algeria. (E-mail: kerdjallel@yahoo.fr)

This article has been accepted for publication in a future issue of this journal, but has not been fully edited. Content may change prior to final publication. Citation information: DOI 10.1109/TPWRD.2019.2943523, IEEE Transactions on Power Delivery

is proposed. It will be demonstrated in this paper that the series LC filter, which is proposed in [10] can be eliminated if the filter is very well designed, and utilizes only the main impedance to force the harmonics to flow into the filter; therefore, defects of the series LC filter are overcomed. Moreover, the modeling of the filter is attained via an equivalent model based on a mathematical development which exhibits the mechanism of the harmonic mitigation. Furthermore, mathematical equations are derived to enhance the filtering capability based on the existing parameters of the main impedance. Although most systems are highly inductive, the effect of resistors on the filtering capability of the FC-TCR compensator cannot be neglected. Therefore, the theoretical analyses and modeling of the filter consider the circuit to be lossy. To obtain better results, a robust control strategy based on the Fixed-Point iteration technique is applied to detect the firing angle (α) of the TCR. This control proved its efficiency in estimating α with accurate information and fast transient response. A practical SPS is selected to ensure and demonstrate the performance of proposed methodology via thorough simulations under MATLAB/Simulink environment.

The rest of the paper is organized as follow. In Section II, the theoretical analyses and the modeling of the proposed compensator are presented. Section III presents the control algorithm of the compensator. Section IV portraits the simulation results, and finally, Section V concludes this study.

II. Circuit Configuration and Design Parameters for the Proposed Compensator

The study case of the the main electrical structure of the modeled electrical power system of the ship is built based on a real electrical power system of a Semi-Submersible Deck Cargo/Heavy Lift Carrier ship that is presented in Fig. 1. It comprises two identical zones, each zone consists of:

- Two fixed speed diesel generators (8725 kVA, 6980 ekW) connected to the switchboard (MVSB 6.6 kV) to feed the ship.
- Two steam tunnel thrusters (1000 kW/1750 kW) connected via soft starter. They are implemented to run lateral maneuverability during the docking of the ship and a high shove at a standstill.
- Two propulsions (4000kW) are used to provide a large thrust to move the ship.
- Two shifted transformers (6.6 kV/715V) to decrease the voltage for the propulsions and attenuate their harmonics.
- Two main thruster converters (715V) are used to vary the speed of the propulsions.
- Three Ballasting pumps (560 kW) are installed to stabilize the ship and ensure its trim and and provide DC power for the electric devices (computers, measurement devices…etc).
- Proposed FC-TCR HF to suppress harmonics, and compensate the power factor.

The rest of the loads are not modeled as they cause negligible power quality issues comparing to the propellers.

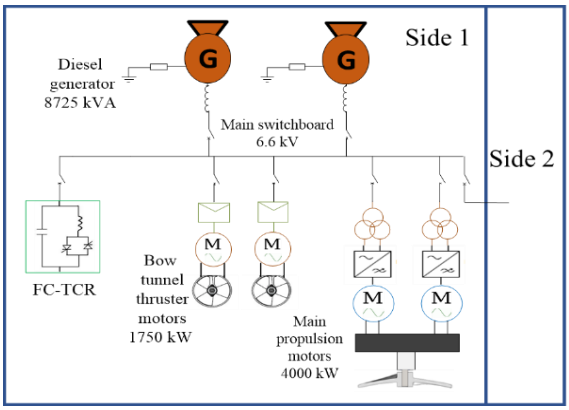

Fig.1. Simplified single-line diagram of the FC-TCR compensator connected to the main switchboard of an all-electic-ship power system

A typical simplified single-line diagaram of all-electric shipboard power system is portrayed in Fig. 1. It comprises two identical sides, each one contains two fixed speed diesel generators, two steam tunnel thrusters, two propellers and other connecting devices. The FC-TCR compensator is added to the main switchboard to mitigate harmonics, compensate the PF, and improve voltage stability. The per-phase single diagram of the FC-TCR compensator is depicted in Fig. 2, in which Fig. 2 (a) portraits the equivalent single-line circuit of Fig. 1. In order to simplify the design of the compensator, the harmonic currents are separated from the non-linear loads and depicted as current sources as presented in Fig. 2 (b), where $i_{Fh5} \dots i_{FhN}$ are the harmonic currents caused by the TCR, and $i_{loh5} \dots i_{lohN}$ are the harmonic currents caused by the non-linear loads. The equivalent harmonic model, which exhibits the mechanism of the harmonic mitigation of the filter, is portraited in Fig. 2 (c). In Fig. 2, the V_S denotes the voltage source of one or more than one shunt connected generators.

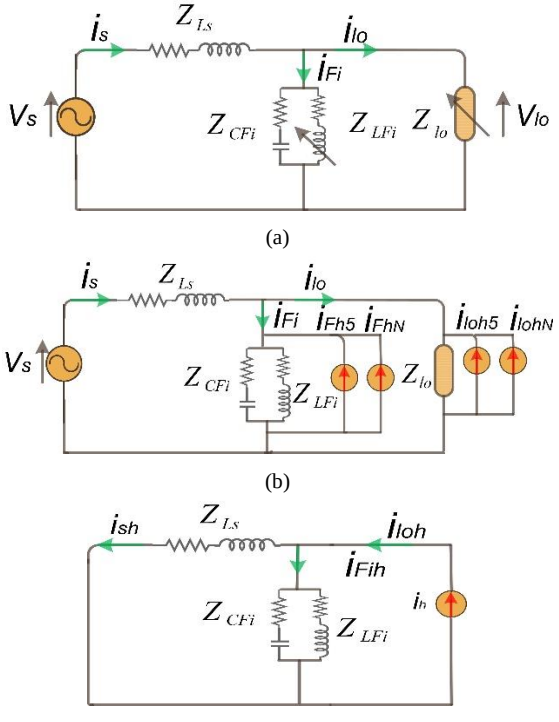

Fig.2. The single-line schematic basic principle of the FC-TCR compensator. (a) The equivalent circuit of FC-TCR compensator for Fig. 1 on a per-phase base form. (b) A simplified version of the circuit depicted in Fig. 2(a). (c) The equivalent harmonic circuit of Fig. 2(a).

This article has been accepted for publication in a future issue of this journal, but has not been fully edited. Content may change prior to final publication. Citation information: DOI 10.1109/TPWRD.2019.2943523, IEEE Transactions on Power Delivery

The V_{lo} is the load voltage and Z_{Ls} is the total main impedance which consists of the sub-transient reactances of the four synchronous generators and transmission line impedance, as it can also include the transformer impedance if it is connected after the generators. The Z_{LFi} and Z_{CFi} are the impedances of the fixed capacitor and the variable reactor of the compensator, respectively. The Z_{lo} is the load impedance, which can be linear or nonlinear such as electric propulsion motors, thruster motors, etc.

The fundamental components can be considered neglected; therefore, V_S is short-circuited, while Z_{lo} is open-circuited, except the source of harmonic currents. i_h denotes the harmonic currents caused by both TCR and non-linear loads. The harmonic currents, which are divided to flow in both the source and the FC-TCR compensator, can be expressed as:

$$\partial = \frac{I_{sh}}{I_{loh}} = \frac{\left| \frac{Z_{LFi} \cdot Z_{CFi}}{Z_{LFi} + Z_{CFi}} \right|}{\left| \frac{Z_{LFi} \cdot Z_{CFi}}{Z_{LFi} + Z_{CFi}} + Z_{Ls} \right|} \tag{1}$$

where $Z_{Ls} = R_{Ls} + X_{Ls}$, $Z_{LFi} = R_{LFi} + X_{LFi}$, and $Z_{CFi} = R_{CFi} + X_{CFi}$. The X_{Ls}, R_{Ls}, X_{LFi}, R_{LFi}, X_{CFi}, R_{CFi} are the reactors and resistances of the main impedance, TCR impedance, and the fixed capacitor, respectively. The ∂ is known as the harmonic attenuation factor which expresses the sharpness of the FC-TCR compensator in terms of filtering [12]. The smaller ∂ is, the higher the filtering performance. Substituting each impedance by its reactors and resistances results in the following formula.

$$\partial = \frac{\left| \frac{(X_{LFi} + R_{LFi}) \cdot (X_{CFi} + R_{CFi})}{X_{LFi} + R_{LFi} + X_{CFi} + R_{CFi}} \right|}{\left| \frac{(X_{LFi} + R_{LFi}) \cdot (X_{CFi} + R_{CFi})}{X_{LFi} + R_{LFi} + X_{CFi} + R_{CFi}} + X_{Ls} + R_{Ls} \right|} \tag{2}$$

After some mathematical manipulations, ∂ becomes as formulated in (3) and (4) at the bottom of this page. In the case where the resistance of the impedances are very small compared to their reactances (lossless system), they can be neglected in the calculation, then (4) can be expressed as:

$$\partial = \frac{1}{\left| 1 + \frac{X_{LFi} \cdot X_{Ls} + X_{CFi} \cdot X_{Ls}}{X_{LFi} \cdot X_{CFi}} \right|} \tag{5}$$

Although, a lossless system benefits from an easier design structure and less complexity. However, in some applications like onshore power systems, due to the medium voltage level and relative smaller ratings of ship power equipment, the resistance effect can be obvious and may not be neglected in the filter design for shipboard power applications.

In practical cases, the number of the connected synchronous generators, which are operated in parallel changes accordingly to the required amount of power. Consequently, The Z_{Ls} changes during this operation. Therefore, in order to provide a high harmonic rejection capability of the FC-TCR HF, the Z_{Ls} should be calculated as the total parallel impedance of the four generators in (1). Thus, effects of the variation of Z_{Ls} are considered in order to ensure that the number of the connecting generators will not affect the filtering capability.

When designing the harmonic filter, the reactors of each impedance should be defined at the first existing dominant harmonic *h* as shown:

$$X_{Ls} = j \cdot L_{Ls} \cdot 2 \cdot \pi \cdot f \cdot h \tag{6}$$

$$X_{LFi} = j \cdot L_{LFi} \cdot 2 \cdot \pi \cdot f \cdot h \tag{7}$$

$$X_{CFi} = \frac{-j}{C \cdot 2 \cdot \pi \cdot f \cdot h} \tag{8}$$

As long as the dominant loads, which cause the perturbation, are three-phase motors, the unbalance is assumed to be very small, thus the existing harmonics are $6h \pm 1$. Therefore, the values of the reactors can be defined at the 5th harmonic during the design of the filter. Since the FC-TCR compensator has the characteristics of a low-pass filter, it will reject the 5th harmonic and all the higher order harmonics. Generally, the shore utility impedance is 3 to 4 times larger than that of transformers [1], [13]. Accurate parameters of Z_{Ls} should be delivered by the vendors to the shipbuilders and filters designers [1]. The current harmonics of the system generally affect V_{lo} by crossing Z_{Ls}. The larger Z_{Ls} is, the higher the distortion of V_{lo}. This issue is proved experimentally in [14], in which the authors demonstrated that the decrease of the redundancy increases the distortion of V_{lo}. However, when implementing the PPFs or the FC-TCR compensator, Z_{Ls} becomes the key factor which forces the harmonic current to flow via the filters, thus both V_{lo} and i_s are filtered. Fig. 3 presents the filtering capability of the FC-TCR compensator in terms of the main and the filter impedances variation. In order to exhibit the influence of the switched capacitor impedance, the parameters of the main impedance are set as $X_{Ls} = 7\ \Omega$ at the fifth harmonic, while $R_{Ls} = 0.5\ \Omega$. According to Fig. 3(a), it is obvious that the

$$\partial = \frac{\left| \frac{X_{LFi} \cdot R_{CFi} + X_{LFi} \cdot X_{CFi} + R_{LFi} \cdot X_{CFi} + R_{LFi} \cdot R_{CFi}}{X_{LFi} + R_{LFi} + X_{CFi} + R_{CFi}} \right|}{\left| \frac{X_{LFi} \cdot R_{CFi} + X_{LFi} \cdot X_{CFi} + R_{LFi} \cdot X_{CFi} + R_{LFi} \cdot R_{CFi}}{X_{LFi} + R_{LFi} + X_{CFi} + R_{CFi}} + X_{Ls} + R_{Ls} \right|} \tag{3}$$

$$\partial = \frac{1}{\left| 1 + \frac{X_{LFi} \cdot X_{Ls} + R_{LFi} \cdot X_{Ls} + X_{CFi} \cdot X_{Ls} + R_{CFi} \cdot X_{Ls} + X_{LFi} \cdot R_{Ls} + R_{LFi} \cdot R_{Ls} + X_{CFi} \cdot R_{Ls} + R_{CFi} \cdot R_{Ls}}{X_{LFi} \cdot R_{CFi} + X_{LFi} \cdot X_{CFi} + R_{LFi} \cdot X_{CFi} + R_{LFi} \cdot R_{CFi}} \right|} \tag{4}$$

This article has been accepted for publication in a future issue of this journal, but has not been fully edited. Content may change prior to final publication. Citation information: DOI 10.1109/TPWRD.2019.2943523, IEEE Transactions on Power Delivery

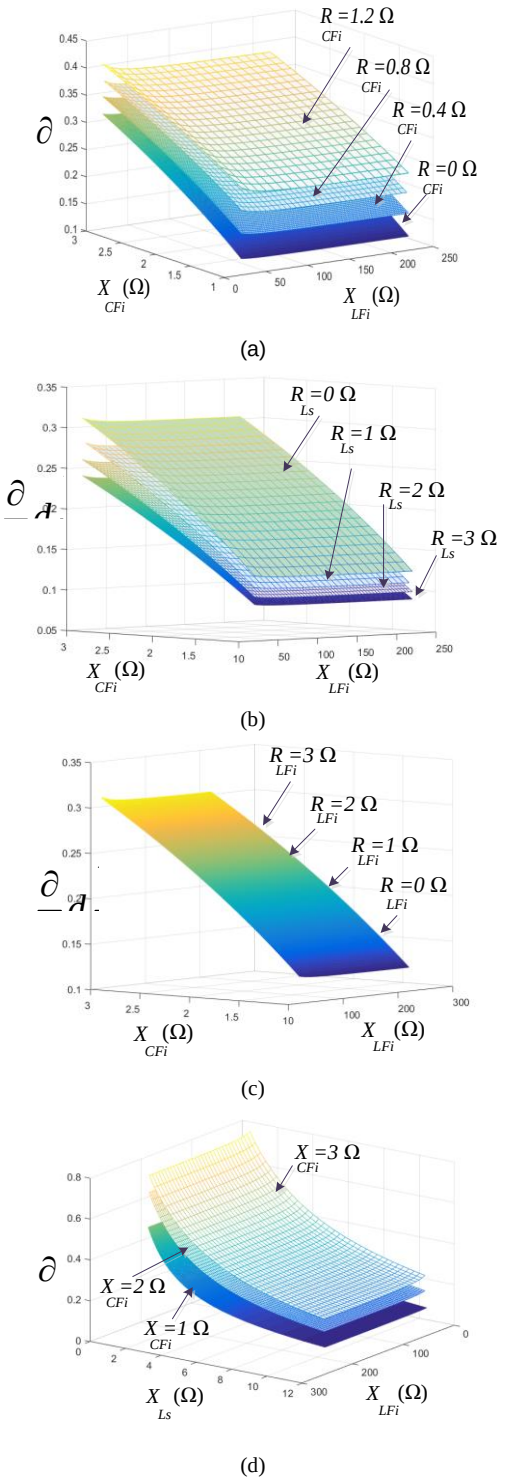

Fig.3. Influence of main and FC-TCR impedances on the filtering performance. (a) Influence of the fixed capacitor resistance in terms of X_{LFi}, X_{CFi} and ∂. (b) Influence of the main impedance resistor in terms of X_{LFi}, X_{CFi} and ∂. (c) the Influence of the TCR resistance in terms of X_{LFi}, X_{CFi} and ∂. (d) Influence of X_{CFi} in terms of X_{Ls}, X_{LFi} and ∂.

decrease of both X_{CFi} and R_{CFi} improves the filter sharpness by decreasing the value of ∂. On the other hand, the variation of X_{LFi} causes a disregarded influence on ∂. Fig. 3(b) portraits the influence of X_{CFi}, X_{LFi} and R_{Ls} in terms of ∂. It can be observed that when the value of X_{CFi} is high, the influence of R_{Ls} is considerable. The larger R_{Ls} is, the smaller ∂ is. When the value of X_{CFi} decreases, the influence of R_{Ls} reduces a bit but still remains significant. Fig. 3(c) presents the influence of R_{LFi} on the performance of the FC-TCR compensator. It is worthy to note that the variation of both R_{LFi} and X_{LFi} does not have any influence on the filtering performance. Fig. 3(d) shows the filtering performance of FC-TCR compensator in terms of X_{CFi}, X_{LFi} and X_{Ls} considering that the system is lossless as presented in equation (5). As mentioned previously, the variation of X_{Ls} occurs due turning ON/OFF the parallel generators. It is obvious that the larger X_{Ls} is, the higher the filtering performance, and the smaller X_{CFi} is the higher filtering performance. While the variation of X_{LFi} provides a negligible effect on ∂. From the four figures depicted in Fig. 3, one can conclude that there is a tradeoff between the rise of Z_{Ls} value and the decrease of Z_{CFi} which optimizes ∂. Therefore, in order to guarantee a high harmonic rejection capability of the FC-TCR compensator, the following equation has to be satisfied:

$$\left|\frac{(X_{LFi}+R_{LFi})\cdot(X_{CFi}+R_{CFi})}{X_{LFi}+R_{LFi}+X_{CFi}+R_{CFi}}\right| << \left|X_{Ls}+R_{Ls}\right| \quad (9)$$

An interesting feature that distinguishes the FC-TCR HF the other hand, the variation of R_{CFi} has a significant dominant and high-order harmonics. In order to confirm the relevance of this assertion, Fig. (4), is depicted. The transfer function of the FC-TCR compensator which is extracted from Fig. 2(a), can be expressed as:

$$G_{FI}^{H}=\frac{V_{lo}}{V_s}=\frac{Z_{Fi}}{Z_{Ls}+Z_{Fi}} \quad (10)$$

where Z_{Fi} is the filter total impedance, substituting *jw* by *s* results in the following formulas:

$$Z_{Ls}=s\cdot L_s+R_{Ls} \quad (11)$$

$$Z_{Fi}=\frac{(s\cdot L_{Fi}+R_{LFi})\cdot(\frac{1}{s\cdot C_{Fi}}+R_{CFi})}{s\cdot L_{Fi}+R_{LFi}+\frac{1}{s\cdot C_{Fi}}+R_{CFi}} \quad (12)$$

$$Z_{Fi}=\frac{s\cdot L_{Fi}+s^2\cdot L_{Fi}\cdot C_{Fi}\cdot R_{CFi}+s\cdot R_{LFi}\cdot R_{CFi}\cdot C_{Fi}+R_{LFi}}{s^2\cdot L_{Fi}\cdot C_{Fi}+s\cdot C_{Fi}(R_{LFi}+R_{CFi})+1} \quad (13)$$

After some mathematical manipulation, Z_{Fi} becomes:

$$Z_{Fi}=\frac{s^2\cdot L_{Fi}\cdot C_{Fi}\cdot R_{CFi}+s\cdot(L_{Fi}+(R_{LFi}\cdot R_{CFi}\cdot C_{Fi}))+R_{LFi}}{s^2\cdot L_{Fi}\cdot C_{Fi}+s\cdot C_{Fi}(R_{LFi}+R_{CFi})+1} \quad (14)$$

Substituting (14) into (10) results in (15). After some mathematical manipulations, (16) is obtained. Equation (16) presents the transfer function of the FC-TCR compensator with the main impedance including their resistors. Based on (16), Fig. 4 is portrayed to show the Bode diagram of the FC-TCR compensator under several scenarios. Fig. 4(a) portraits the Bode diagram of the FC-TCR compensator under different values of the resistors and the reactors of the main impedance. It is clear that the rise of R_{Ls} results in an equal reduction of all frequencies including the fundamental, while the rise of L_s improves the filtering capability relatively with

This article has been accepted for publication in a future issue of this journal, but has not been fully edited. Content may change prior to final publication. Citation information: DOI 10.1109/TPWRD.2019.2943523, IEEE Transactions on Power Delivery

$$G_{FI}^{H}=\frac{1}{1+\dfrac{s^3\cdot L_{Fi}\cdot C_{Fi}\cdot L_s+s^2\cdot C_{Fi}\cdot L_s(R_{LFi}+R_{CFi})+s\cdot L_s+s^2\cdot C_{Fi}\cdot L_{FI}\cdot R_{Ls}+s\cdot C_{Fi}\cdot R_{Ls}(R_{LFi}+R_{CFi})+R_{Ls}}{s^2\cdot L_{Fi}\cdot C_{Fi}\cdot R_{CFi}+s\cdot(L_{Fi}+(R_{LFi}\cdot R_{CFi}\cdot C_{Fi}))+R_{LFi}}} \tag{15}$$

$$G_{FI}^{H}=\frac{1}{1+\dfrac{s^3\cdot L_{Fi}\cdot C_{Fi}\cdot L_s+s^2\cdot(L_s\cdot C_{Fi}(R_{LFi}+R_{CFi})+L_{Fi}\cdot C_{Fi}\cdot R_{Ls})+s\cdot(L_s+C_{Fi}\cdot R_{Ls}\cdot(R_{LFi}+R_{CFi}))+R_{Ls}}{s^2\cdot L_{Fi}\cdot C_{Fi}\cdot R_{CFi}+s\cdot(L_{Fi}+(R_{LFi}\cdot R_{CFi}\cdot C_{Fi}))+R_{LFi}}} \tag{16}$$

the increase of the harmonic order as formulated in (6). Based on these marks, one can deduce that L_s plays an important role in forcing the harmonics to flow through the filter, while R_{Ls} can also prevent the harmonic from flowing into the utility supply. However, the increase of R_{Ls} results in a significant voltage drop and high losses. A confirmation analysis of this assertion is conducted in the simulation results in section IV. Therefore, it is important for the reactor of the main impedance to be dominant ($X_{Ls} >> R_{Ls}$). Fig. 4(b) presents the performance of the FC-TCR compensators in terms of fixed capacitor impedance. It is noteworthy that the increase of C_{Fi} results in more reactive power, thus at low frequencies there is an augmentation gain caused by the resonance between the main impedance and the filter capacitor. Therefore, the capacitors are usually implemented to sustain the stability of the voltage in case of voltage sags caused by heavy loads. However, at high frequencies, both values of the capacitors produce the same filtering gain. On the other hand, the variation of R_{CFi} has a significant influence on attenuating the filtering capability. The larger R_{CFi} is, the lower the performance of the filter. Therefore, based on (16) and Fig. 4(b) one can infer that ensuring a lower resistance of the fixed capacitor results in a high filtering capability. Fig. 4(c) depicts the behavior of the FC-TCR compensator in terms of TCR impedance. It is clear that the increase of R_{LFi} reduces the voltage sags under low frequencies, as well as mitigate the overshoots. However, the variation of the L_{Fi} during adjusting the PF does not affect the filtering performance. Therefore, the control of TCR for compensating the PF is not constrained to the filtering capability.

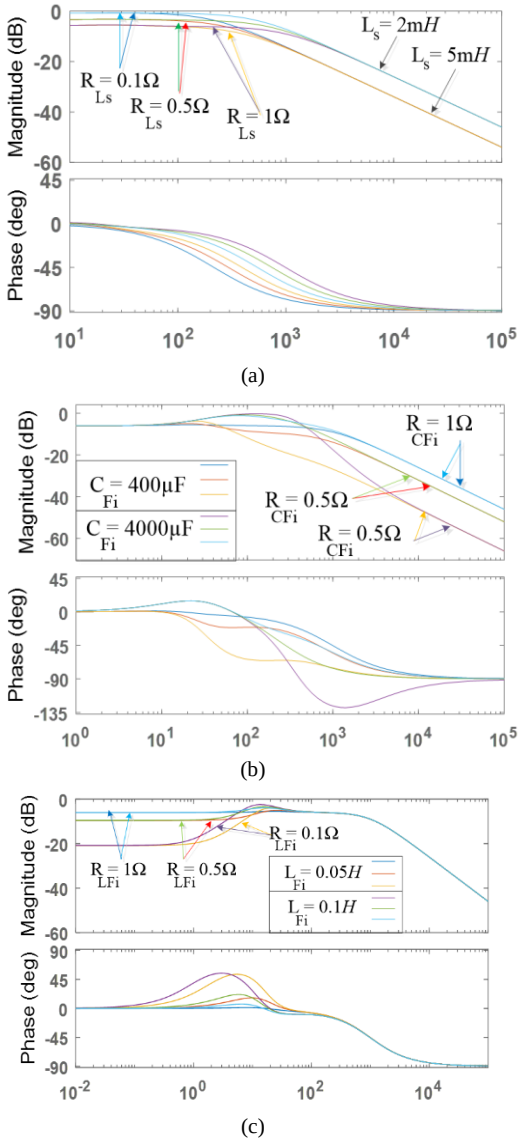

Fig.4. Bode diagram of the FC-TCR compensator. (a) effects of main impedance on the filtering capability. (b) effects of the switched capacitor impedance in the filtering capability. (c) effect of the TCR impedance on the filtering capability.

Fig. 5 is presented to facilitate the procedures of designing the FC-TCR compensator to act as a low-pass filter. The flowchart starts with the identification of the parameters of the main impedance of the ship and the parameters of the FC-TCR compensators that are available in the market. Then the filtering capability of the FC-TCR compensator is obtained

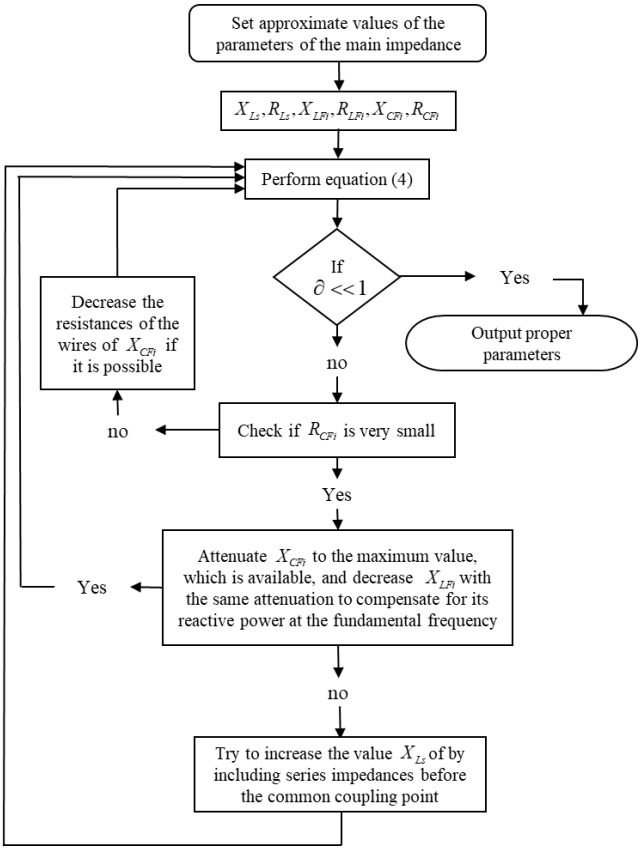

Fig.5. Procedures of choosing the right parameters to enable the FC-TCR compensator to act as a low-pass filter.

This article has been accepted for publication in a future issue of this journal, but has not been fully edited. Content may change prior to final publication. Citation information: DOI 10.1109/TPWRD.2019.2943523, IEEE Transactions on Power Delivery

by estimation ∂ using (4). If ∂ is small enough to provide a good harmonic attenuation (for a THD of around 30% to 40% of both voltage and current, ∂ should be less than 0.2), then the engineers can use these parameters. If ∂ is not smaller enough, then the engineers try to mitigate the resistance of the wires that connect the switched capacitor to the main switchboard. If ∂ remains larger than the desired value, the engineers should decrease the impedance of the reactance of the switched capacitor to decrease the bandwidth of the filter as presented in Fig. 4. It is noteworthy to remark that when decreasing X_{CFi}, more capacitive reactive power will be injected into the system. Therefore, the designers must make sure that the reactor of the TCR can compensate for all these capacitive reactive power under a different operating mode of the ship. In the worst case, if ∂ remains larger than the desired value, then the engineers can increase X_{Ls} by adding extract impedance before the common coupling point and make sure that these values do not cause an important voltage drop.

III. Control Method of the FC-TCR Compensator

Static var compensators (SVC) with TCRs have been growing fast due to their low cost, and high performance in several applications [15], [16]. The basic structure of an FC-TCR compensator comprises a fixed capacitor in parallel with a variable reactor, this latter contains two anti-parallel sophisticated valves which work alternatively each half-cycle [17]. The fixed capacitor compensates for the lagging power factor and generates extra capacitive reactive power, then the TCR adjusts the leading power factor to be near to unity. The firing angle α defines the amount of reactive power which is generated by the FC-TCR compensator, and it is estimated by the following formula.

$$-2\alpha+\sin(2\alpha)-2\pi=\pi\frac{L_{FI}}{L_{FI}(\alpha)} \tag{17}$$

where L_{Fi} is the real value of the TCR inductance and $L_{Fi}(\alpha)$ is the new inductance obtained by adjusting α. As long as (17) is a non-linear equation, the solution cannot be obtained directly. Generally, the linearization of (17) is achieved by an offline calculation based on a lookup table which is stored in the microprocessor [17]. However, this technique shows a low accuracy under voltages sags and frequency drifts. The Fixed-Point iteration technique can be performed online and provides an accurate approximation of estimating α, thus this technique is adaptive and provides high performance even under frequency drifts. Fig. 6 presents the control algorithm of the FC-TCR compensator, which is an open-loop technique. In contradiction with the control used in [10] which is a closed-loop technique, the open-loop technique is distinguished by the simplicity (does not require stability analyzes or controller design), and fast dynamic response. According to Fig. 6, the discrete Fourier transform (DFT) is applied to estimate the magnitudes and phase angles of V_{lo}, I_s and the filter current I_{fi}. Then the magnitude of I_s is multiplied by sin(ϕ) to obtain accurate information about the reactive current flowing inside the system. The DFT is

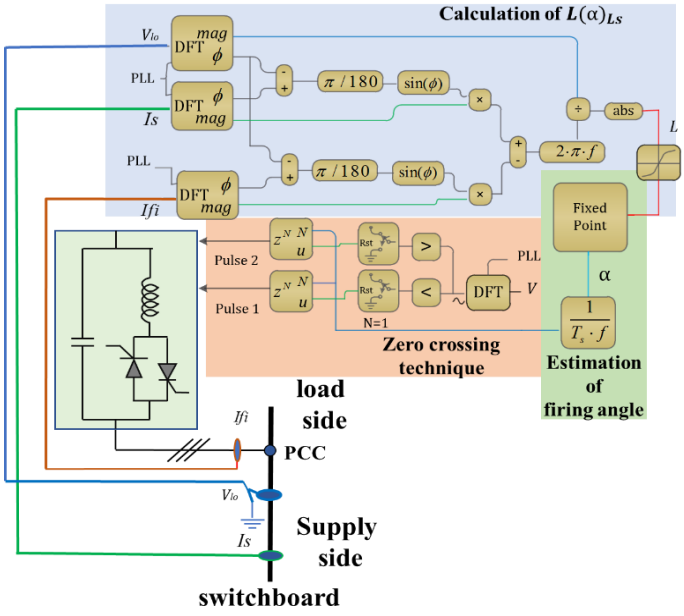

Fig.6. Single-line diagram of FC-TCR based control algorithm.

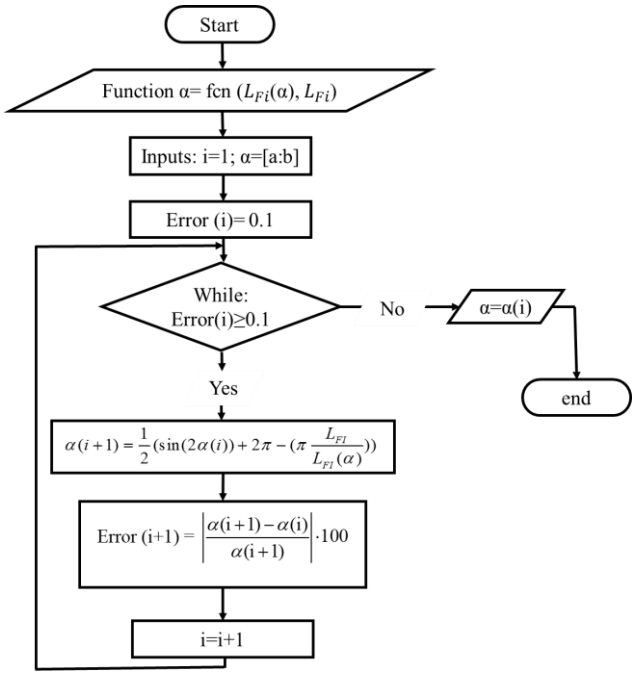

Fig.7. Flowchart of fixed point technique for estimating the firing angle α.

adapted with the phase-locked loop (PLL) to provide accurate estimation under frequency drifts. In real applications, the sensors of current are located inside each connected generators. Since the proposed compensator is connected at the point of the common coupling (PCC), where in general it is the main switching board, the load current I_{lo} can not be sensed. Adding extra sensors on the main switchboard increases the complexity and the cost of the system. This issue, however, can be avoided by sensing the current of the FC-TCR HF I_{fi} and the current of each generators, then subtract them from each other as shown below:

$$I_{lo}=I_s-I_{fi} \tag{18}$$

where I_s is the sum of the source currents of the connected generators. After that, the inductance which is supplied by the TCR can be calculated as:

This article has been accepted for publication in a future issue of this journal, but has not been fully edited. Content may change prior to final publication. Citation information: DOI 10.1109/TPWRD.2019.2943523, IEEE Transactions on Power Delivery

$$L_{Fi}(\alpha) = \frac{V_{lo}}{2 \cdot \pi \cdot f \cdot I_{in}} \tag{19}$$

where I_{in} is the reactive current which is flowing in the system. After defining $L_{Fi}(\alpha)$, the estimation of α is attained based on the Fixed-Point iteration technique using equation (17) and the proposed flowchart depicted in Fig. 7.

where α (i) and Error (i) are the initial guests of α and the allowable approximation error, [a:b] and [c:d] are respectively the boundaries of α and Error. For the sake of the simplicity, let us consider x= $\alpha(i+1)$ and $g(\alpha(i)) = \frac{1}{2}(\sin(2\alpha(i)) + 2\pi - (\pi \frac{L_{FI}}{L_{FI}(\alpha)}))$, according to the theorem of the Fixed-Point iteration technique, in order to ensure the convergence of the function to the unique fixed point, the following condition has to be satisfied:

$$\left|g'(\alpha(i))\right| \le k < 1. \ \forall \ \alpha \in [a,b] \tag{20}$$

where $g'(\alpha(i))$ is the derivative of $g(\alpha(i))$ with $g'(\alpha(i))$ and $g(\alpha(i)) \in [a,b]$. Note that $g'(\alpha(i)) = \cos(2\alpha(i))$, as long as for the star connection of the FC-TCR compensator, $\alpha(i)$ is confined between $\frac{\pi}{2} < \alpha(i) < \pi$, this implies that the algorithm always converges.

IV. Numerical Analysis and Discussion

The simulated model is developed under MATLAB/Simulink environment in accordance with the schematic presented in Fig. 1. The main system parameters are listed in Table I. Four study cases are cosidered and analyzed:

A. *Case study 1: Dynamic response of the FC-TCR compensator in filtering harmonics and compensating the PF under load variation*.

Fig. 8 demonstrates the capability of the FC-TCR compensator in suppressing harmonics and improving the power factor under load variations. Before connecting the FC-TCR compensator, the THDs of both V_{lo} and I_s are respectively 42% and 10% which do not respect the IEC61000-3-6 and IEEE Std 519™-2014 standards, and the PF is around 0.82. The fact that the THD of V_{lo} is much higher than I_s is because the harmonic currents have jumped into the voltage through the main impedance. The THDs are a bit exaggerated to demonstrate the performance of the FC-TCR compensator under the worst cases of contamination. In the instance 0.06s, the switched capacitor is connected. Since this latter is calculated to provide a large amount of capacitive reactive power, it drives the lagging PF toward a leading PF by crossing the unity. Moreover, based on equation (9), the connection of the switched capacitor has improved the waveform of both V_{lo} and I_s to less than 5% which conforms to the aforementioned norms. It is noteworthy to observe that V_{lo} is increased when connecting the switched capacitor, this phenomenon occurs due to the resonance between the main impedance and the switched capacitor.

TABLE I
SYSTEM PARAMETERS

Category	Parameters	Values
Synchronous generators	Nominal voltage	V=6.6 kV (+6%, -10%)
	Electric Power	P=6980 ekW,
	Apparent power	S=8725 kVA,
propellers	Rated power	P=4000 kW
thrusters	Rated power	P=1750 kW
Shifted Transformers	Transformed voltage	V=6.6 kV/715V
Non-linear loads	Rated power	P=700kW
FC-TCR compensator	Main impedance	$L_{Ls} = 0.006\ H\ \ R_{Ls} = 0.5\ \Omega$
	Switched capacitor	$L_{Fi} = 450\ \eta F\ \ R_{CFi} = 0.5\ \Omega$
	TCR inductor	$L_{Fi} = 5\ mH\ \ R_{LFi} = 0.5\ \Omega$

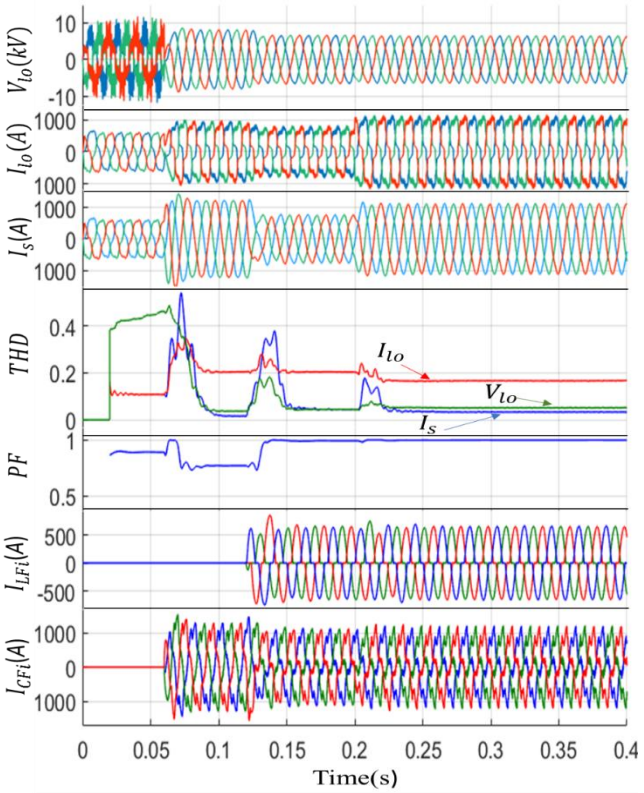

Fig.8. Dynamic response of FC-TCR compensator in filtering harmonics and compensating power factor under 50% of loading.

Therefore, the capacitors are implemented to improve the voltage stability in several applications which suffer from voltage sags. In the instance 0.12s, the TCR is connected. It is clear that the TCR pushes the PF near to unity without affecting the waveform of both V_{lo} and I_s, and thus validates the analyses provided in section II, and the illustration of Fig. 3(c). In the instance 0.24s, a loading of 50% occurs. It is observable that the dynamic response of the FC-TCR compensator in terms of harmonic filtering and PF compensation is very fast (less than a cycle).

B. *Study case 2: the influence of the switched capacitor resistance on the harmonic filtering performance of the FC-TCR compensator*.

Fig. 9 depicts the behavior of the FC-TCR HF under different values of R_{CFi}. In the instance 0.6 s, the switched capacitor is connected. According to equation (4), setting

This article has been accepted for publication in a future issue of this journal, but has not been fully edited. Content may change prior to final publication. Citation information: DOI 10.1109/TPWRD.2019.2943523, IEEE Transactions on Power Delivery

R_{CFi} =5 Ω does not provide a sufficient decrease of ∂, thus the THD of V_{lo} decreases from 42% to 10% which does not conform to the norms. Moreover, the increase of R_{CFi} results in absorbing more active power and decreases the amount of capacitive reactive power generated by X_{CFi}. Reducing R_{CFi} to 2 Ω in the instance 0.16s results in decreasing the active power absorbed by the compensator, and decreases the THD of V_{lo} to around 7%. Finally, setting R_{CFi} to 0.5 Ω results in an acceptable THDs of both V_{lo} and I_s (less than 5%), and absorbs less active power. Notice that the PF is improved by the TCR to be near to unity. These results are an adequate prove which validates equation (4), and the study analyses which are depicted in Fig. 3 (a) and Fig 4 (b).

C. *Study case 3: the influence of the main impedance resistance on the harmonic filtering performance of the FC-TCR compensator.*

Fig. 10 presents the influence of R_{Ls} on the FC-TCR HF. The connection of the switched capacitor in the instance 0.06 s decreases the THDs of V_{lo} and I_s to less than 5%, then in the instance 0.12 s the TCR is connected. However, setting R_{Ls} to 5 Ω results in a severe drop voltage, and causes a larger dynamic response in compensating the PF. Then, in the second stage (0.16 s), the decrease of R_{Ls} improves the voltage sag. Finally, setting R_{Ls} to 0.5 Ω in the instance 0.24 s results in an acceptable voltage sag, and improves the dynamic response of the FC-TCR in compensating the PF near to unity. According to the IEEE std. 45 [18], IEC std. 60092-101 [19], ABS rule [20], and Polish Register of Shipping rule [21] standards, the voltage magnitude of the electrical power system onboard should be in the range of +6% and -10%. It is remarkable that in all stages, the THDs

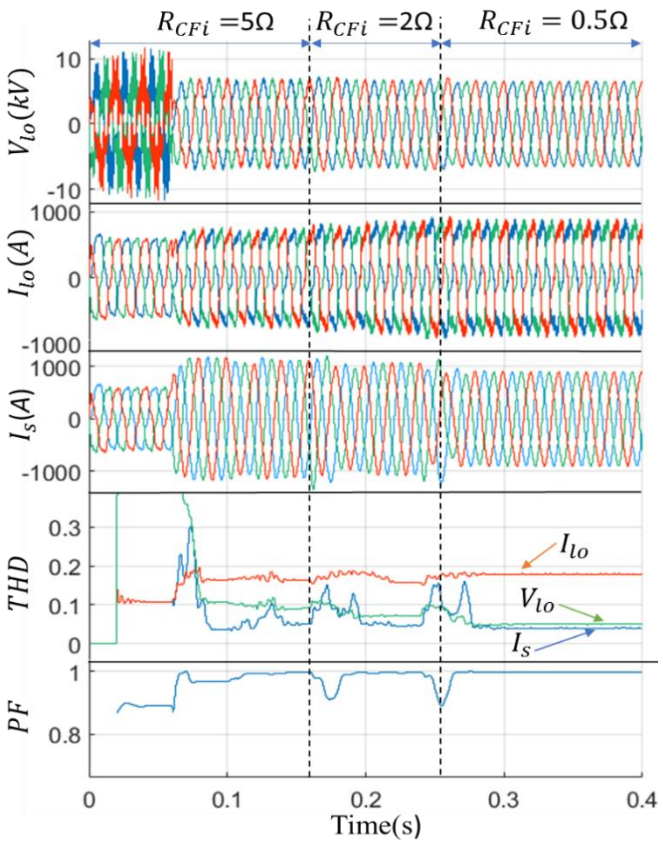

Fig.9. Influence of the switched capacitor resistance on the behavior of the FC-TCR compensator.

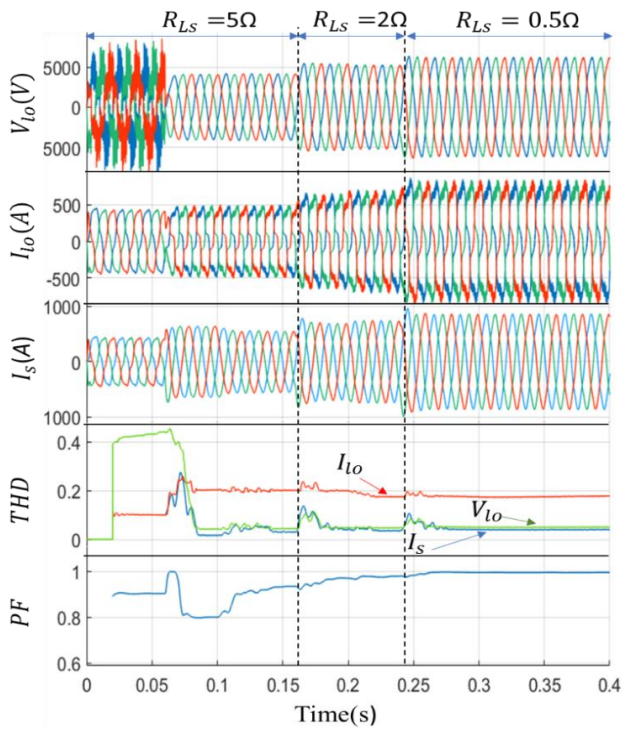

Fig.10. Influence of main impedance resistance on the behavior of the FC-TCR compensator.

of both V_{lo} and I_s are less than 5 %. Based on these results, one can deduce that the increase of R_{Ls} improves the filtering performance of the FC-TCR compensator as demonstrated in theoretical analyses in Section II, Fig. 3(b) and Fig. 4(a). On the other hand, the increase of R_{Ls} causes a voltage sag. Therefore, when designing the filter, it is mandatory to ensure that $R_{Ls} << X_{Ls}$ so that R_{Ls} can be neglected.

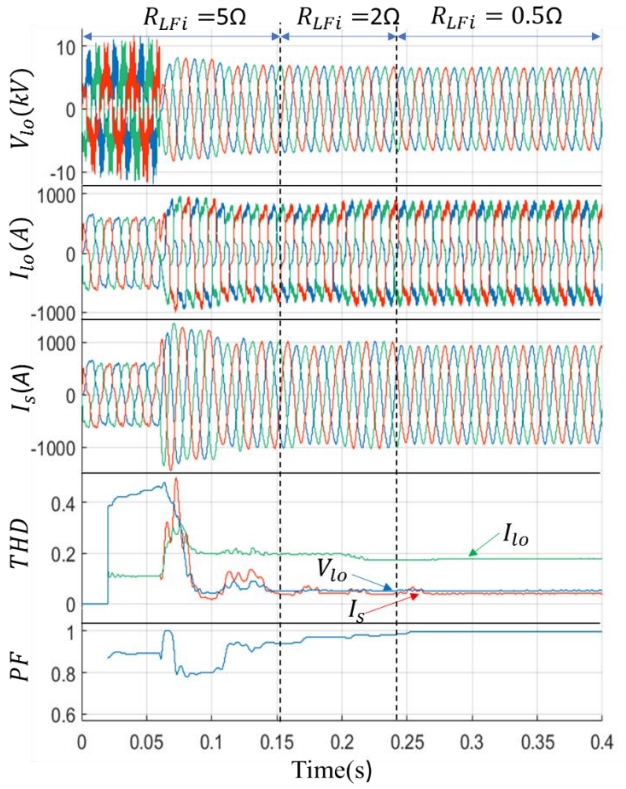

Fig.11. Influence of main impedance resistance on the behavior of the FC-TCR compensator.

D. *Study case 4: influence of the TCR resistance on the harmonic filtering performance of the FC-TCR compensator.*

Fig. 11 depicts the influence of the R_{LFi} on the behavior of the FC-TCR HF. It is observable that the TCR provides less accuracy in compensating the PF in the first stage (0.12s) when R_{LFi} is set to 5 Ω. Reducing R_{LFi} to 2 Ω results in more accuracy of compensating the PF. Finally, in the last stage, setting R_{LFi} to 0.5 Ω enables the FC-TCR to compensate the PF accurately. It is noteworthy to remark that the change of R_{LFi} does not affect the filtering capability of the FC-TCR, this is a sufficient prove which validates equations (4) and (15) and the theoretical analyses which are provided in section II and portrayed in Figs. 3(c) and 4(c).

V. CONCLUSION

In this paper, a cost-effective compensator based on FC-TCR has been proposed for all-electric shipboard power systems. In order to effectively suppress harmonics and compensate power factor, the theoretical analyses and mathematical equations for the FC-TCR compensator have been developed. The developed equivalent lossy circuits which exhibit the mechanism of the harmonic suppression have been presented to facilitate the design of the compensator. The Fixed-Point iteration technique is also used to extract the firing angle of the TCR with more accuracy and faster dynamic response. Based on the conducted results, the proposed topology can present the following advantages:

- Wide range selectivity: using the proposed design approach, the FC-TCR can select a wide range of the frequency components, including the dominant ones, to be suppressed. In opposition to the traditional passive power filters that require a single tuned filter for each aimed harmonic to be filtered.
- Negligible switching loss: in contradiction with the advanced solutions based on power inverters such as the active power filters that often demand an operation at high switching frequencies, the FC-TCR compensator needs only one pulse every half cycle. It means that the switching losses in the proposed filter are significantly reduced.
- High harmonic filtering capability: in contrast with the conventional solutions such as passive and active power filters, whose filtering performance degrades at high order harmonics due to their confined selectivity (for passive power filters) and the limited switched frequency (for the active power filters). The proposed filter can act as a low-pass filter; hence, filter all the high order harmonics.
- A low-cost solution: Compared to the conventional techniques, which are often based on power converters and demand a high implementation cost, the proposed method is a low-cost solution as it only requires one passive filter and one thyristor.

The proposed method is verified by thorough simulations of a practical ship power system under different operating conditions. The proposed filter design model can provide the advantages in terms of wide range selectivity, negligible switching loss, high harmonic filtering capability, and a low-cost solution as compared to the traditional method. Attention is paid to use of the proposed method in considering to conduct an appropriate experimental verification of the results. Experimental research using scale models is one way of making better use of knowledge about the problem under study. Exactly what form that existing system voltage and demand power will determine what kind of experimental technique can be used. The validation of proposed method with potential complementary experiments using manufactured scale models for all-electric shipboard power systems is the subject for future study.

REFERENCES

[1] Control of Harmonics in Electrical Power Systems, American Bureau of Shipping Guidance, 2006.

[2] S. Jayasinghe, L. Meegahapola, N. Fernando, Z. Jin, and J. Guerrero, "Review of Ship Microgrids: System Architectures, Storage Technologies and Power Quality Aspects," *Inventions*, vol. 2, no. 1, p. 4, 2017.

[3] G. Sulligoi, A. Vicenzutti, V. Arcidiacono, and Y. Khersonsky, "Voltage Stability in Large Marine Integrated Electrical and Electronic Power Systems," *IEEE Trans. Ind. Appl.*, vol. 9994, no. c, pp. 1–1, 2016.

[4] J. Mindykowski, "Power quality on ships: Today and tomorrow's challenges," *EPE 2014 - Proc. 2014 Int. Conf. Expo. Electr. Power Eng.*, no. December 2014, pp. 1–18, 2014.

[5] Terriche, Yacine, et al. "An Effective and Low-Cost Passive Compensator System to improve the Power Quality of Two Electric Generators." IET Power Electronics (2019).

[6] S. V. Giannoutsos and S. N. Manias, "A Systematic Power-Quality Assessment and Harmonic Filter Design Methodology for Variable-Frequency Drive Application in Marine Vessels," *IEEE Trans. Ind. Appl.*, vol. 51, no. 2, pp. 1909–1919, Mar. 2015.

[7] Y. Li *et al.*, "A controllably inductive filtering method with transformer-integrated linear reactor for power quality improvement of shipboard power system," *IEEE Trans. Power Deliv.*, vol. 32, no. 4, pp. 1817–1827, 2017.

[8] Y. Terriche, S. Golestan, J. M. Guerrero, D. Kerdoune, and J. C. Vasquez, "Matrix pencil method-based reference current generation for shunt active power filters," *IET Power Electron.*, vol. 11, no. 4, pp. 772–780, Apr. 2018.

[9] An Luo, Zhikang Shuai, Wenji Zhu, Ruixiang Fan, and Chunming Tu, "Development of Hybrid Active Power Filter Based on the Adaptive Fuzzy Dividing Frequency-Control Method," *IEEE Trans. Power Deliv.*, vol. 24, no. 1, pp. 424–432, Jan. 2009.

[10] A. Hamadi, S. Rahmani, and K. Al-Haddad, "A hybrid passive filter configuration for VAR control and harmonic compensation," *IEEE Trans. Ind. Electron.*, vol. 57, no. 7, pp. 2419–2434, 2010.

[11] L. Wang, C. Lam, M. Wong, N. Dai, K. Lao, and C. Wong, "Non-linear adaptive hysteresis band pulse- width modulation control for hybrid active power filters to reduce switching loss," vol. 8, pp. 2156–2167, 2015.

[12] Na He, Dianguo Xu, and L. Huang, "The Application of Particle Swarm Optimization to Passive and Hybrid Active Power Filter Design," *IEEE Trans. Ind. Electron.*, vol. 56, no. 8, pp. 2841–2851, Aug. 2009.

[13] R. M. S. Q. Mary, "RMS Queen Mary 2 Report No 28/2011.," no. 28, 2011.

[14] T. Tarasiuk, A. Pilat, and M. Szweda, "Experimental study on impact of ship electric power plant configuration on power quality in the ship power system," *Lect. Notes Eng. Comput. Sci.*, vol. 1, 2014.

[15] J. R. C. Orillaza and A. R. Wood, "Harmonic State-Space Model of a Controlled TCR," *IEEE Trans. Power Deliv.*, vol. 28, no. 1, pp. 197–205, Jan. 2013.

[16] S. Das, D. Chatterjee, and S. K. Goswami, "A GSA-Based Modified SVC Switching Scheme for Load Balancing and Source Power Factor Improvement," *IEEE Trans. Power Deliv.*, vol. 31, no. 5, pp. 2072–2082, Oct. 2016.

[17] R. M. Mathur and R. K. Varma, *Thyristor-based FACTS controllers for electrical transmission systems*. John Wiley & Sons, 2002.

[18] *IEEE recommended practice for electrical installations on shipboard*, IEEE Standard 45–2002.

[19] IEC Standard 60 092-101-2002, Electrical installations in ships. Definitions and general requirement, 2002

[20] Rules for Building and Classing Steel Vessels, American Bureau of Shipping, Houston, TX, USA, 2008.

This article has been accepted for publication in a future issue of this journal, but has not been fully edited. Content may change prior to final publication. Citation information: DOI 10.1109/TPWRD.2019.2943523, IEEE Transactions on Power Delivery

[21] Statków, Polski Rejestr. "Technical Requirements for Shipboard Power Electronic Systems." Polish Register of Shipping: Gdansk, Poland, 2006.

BIOGRAPHIES

Yacine Terriche received the B.S. degree in electrical engineering from University of scienice and Technology, Consatantine, Algeria in 2011, and the M.S. degree in Electrical Engineering from University of Constantine 1, Constantine, Algeria. in 2013. He is currently working towards the Ph.D. degree at the Department of Energy Technology, Aalborg University, Denmark. His research interests include power electronics, modeling, control, signal processing, power quality issues, active and passive power filters, and shipboard Microgrids.

Muhammad Umair Mutarraf received the B.Sc. degree in electrical engineering from University of Engineering and Technology, Lahore, Pakistan in 2013, and the MEng. degree in Control Theory & Control Engineering from Xidian University, China in 2017. He is currently working towards the Ph.D. degree at the Department of Energy Technology, Aalborg University, Denmark. His research interests include power electronics, modeling, control and integration of energy storages in AC & DC shipboard Microgrids.

Saeed Golestan (M'11-SM'15) received the B.Sc. degree in electrical engineering from Shahid Chamran University of Ahvaz, Iran, in 2006, the MSc degree in electrical engineering from the Amirkabir University of Technology, Tehran, Iran, in 2009, and the PhD degree in electrical engineering from Aalborg University, Aalborg, Denmark, in 2018.

He is currently an assistant professor at the Department of Energy Technology, Aalborg University, Denmark. His research interests include synchronization and signal processing techniques in power applications, and modeling and control of power converters.

Chun-Lien Su (M'01-SM'13) received the Diploma degree in Electrical Engineering from National Kaohsiung Institute of Technology, Taiwan, the M.S. and Ph.D. degrees in Electrical Engineering from the National Sun Yat-Sen University, Taiwan in 1992, 1997, and 2001, respectively.

In 2002 and 2006, he was Assistant Professor and Associate Professor at the Department of Marine Engineering, National Kaohsiung Marine University, Taiwan, respectively. Since 2012, he has been as a Full Professor where he is the Director at the Energy and Control Research Center. From Aug. 2017 to Jan. 2018 he was a Visiting Professor at the Department of Energy Technology, Aalborg University, Denmark and is now Professor in National Kaohsiung University of Science and Technology. His research interests include power system analysis and computing, power quality, maritime microgrids, and offshore energy; recently specially focused on electrical infrastructure for offshore wind farms and maritime microgrids for electrical ships, vessels, ferries and seaports.

Dr. Su was a recipient of the best paper prize of the Industrial & Commercial Power Systems Conference at IEEE-IAS for the period 2012-2013, and the best paper award of IEEE International Conference on Smart Grid and Clean Energy Technologies in 2018. He is a Guest Editor of the IEEE TRANSACTIONS ON INDUSTRIAL INFORMATICS SPECIAL ISSUES: NEXT GENERATION INTELLIGENT MARITIME GRIDS and IET RENEWABLE POWER GENERATION SPECIAL ISSUES: POWER QUALITY AND PROTECTION IN RENEWABLE ENERGY SYSTEMS AND MICROGRIDS.

Josep M. Guerrero (S'01-M'04-SM'08-FM'15) received the B.S. degree in telecommunications engineering, the M.S. degree in electronics engineering, and the Ph.D. degree in power electronics from the Technical University of Catalonia, Barcelona, in 1997, 2000 and 2003, respectively. Since 2011, he has been a Full Professor with the Department of Energy Technology, Aalborg University, Denmark, where he is responsible for the Microgrid Research Program (www.microgrids.et.aau.dk). From 2014 he is chair Professor in Shandong University; from 2015 he is a distinguished guest Professor in Hunan University; and from 2016 he is a visiting professor fellow at Aston University, UK, and a guest Professor at the Nanjing University of Posts and Telecommunications. From 2019 he became a Villum Investigator.

His research interests is oriented to different microgrid aspects, including power electronics, distributed energy-storage systems, hierarchical and cooperative control, energy management systems, smart metering and the internet of things for AC/DC microgrid clusters and islanded minigrids; recently specially focused on maritime microgrids for electrical ships, vessels, ferries and seaports. Prof. Guerrero is an Associate Editor for a number of IEEE TRANSACTIONS. He has published more than 500 journal papers in the fields of microgrids and renewable energy systems, which are cited more than 30,000 times. He received the best paper award of the IEEE Transactions on Energy Conversion for the period 2014-2015, and the best paper prize of IEEE-PES in 2015. As well, he received the best paper award of the Journal of Power Electronics in 2016. During five consecutive years, from 2014 to 2018, he was awarded by Clarivate Analytics (former Thomson Reuters) as Highly Cited Researcher. In 2015 he was elevated as IEEE Fellow for his contributions on "distributed power systems and microgrids."

Juan C. Vasquez (M'12-SM'14) received the B.S. degree in electronics engineering from the Autonomous University of Manizales, Manizales, Colombia, and the Ph.D. degree in automatic control, robotics, and computer vision from BarcelonaTech-UPC, Spain, in 2004 and 2009, respectively. He was with the Autonomous University of Manizales working as a teaching assistant and the Technical University of Catalonia as a Post-Doctoral Assistant in 2005 and 2008. In 2011, He was Assistant Professor and in 2014 He was an Associate Professor at the Department of Energy Technology, Aalborg University, Denmark. In 2019, He became a Full Professor and currently He is the Vice Programme Leader of the Microgrids Research Program (see microgrids.et.aau.dk). He was a Visiting Scholar at the Center of Power Electronics Systems (CPES) at Virginia Tech and a visiting professor at Ritsumeikan University, Japan. His current research interests include operation, advanced hierarchical and cooperative control, optimization and energy management applied to distributed generation in AC/DC Microgrids, maritime microgrids, advanced metering infrastructures and the integration of Internet of Things and Energy Internet into the SmartGrid. Dr Vasquez is a Associate Editor of IET POWER ELECTRONICS and a Guest Editor of the IEEE TRANSACTIONS ON INDUSTRIAL INFORMATICS Special Issue on Energy Internet. In 2017 and 2018, Dr. Vasquez was awarded as Highly Cited Researcher by Thomson Reuters and in 2019, He was the recipient of the Young Investigator Award 2019. He has published more than 300 journal papers in the field of Microgrids, which in total are cited more than 15000 times. Dr. Vasquez is currently a member of the IEC System Evaluation Group SEG4 on LVDC Distribution and Safety for use in Developed and Developing Economies, the Renewable Energy Systems Technical Committee TC-RES in IEEE Industrial Electronics, PELS, IAS, and PES Societies.

This article has been accepted for publication in a future issue of this journal, but has not been fully edited. Content may change prior to final publication. Citation information: DOI 10.1109/TPWRD.2019.2943523, IEEE Transactions on Power Delivery

Djallel Kerdoun received the B. Sc. Degree and M. Sc. degree in electrical drive and automation of industrial and technological complexes from the Technical University, Institute of Energy of Moscow, Russia, in 1995 and 1997, respectively. And he received the Ph.D. degree in electrical engineering from the Technical University, Institute of Energy of Moscow, Russia, in 2001 for his work on Asynchronous Electric Drive of Spherical Drum-Type Mills with use of Voltage Regulator.

Since 2004, he has been with the Department of Electrical Engineering, The University of Constantine1, Constantine, Algeria, first as a Research Assistant, then as a Lecturer in power electronic systems, with the Power electronics, Machines, and Control Group. Recently he has become the head of the departement of the Electrical Engineering at The University of Constantine1, Constantine, Algeria.

His research interests include Solid State Drives, Power Converters, Electrical Machines, and Wind and Photovoltaic Power Generation.